01

Collisional-radiative recombination of Ne^{++} and Ne^{+} ions with electrons in the decaying plasma of a low-pressure barrier discharge

© *V.A. Ivanov*

St. Petersburg State University,
198504 St. Petersburg, Russia

e-mail: v.a.ivanov@spbu.ru

Received December 24, 2021
Revised February 13, 2022
Accepted April 6, 2022

The results of an experimental study and simulation of radiation generated by the processes of collisional-radiative recombination of neon ions Ne^{+} and Ne^{++} with electrons of the decaying plasma are presented. Plasma was created by a barrier discharge in a cylindrical glass tube with electrodes on its surface. Experimental conditions: neon pressure 0.65 Torr, electron density at the initial stage of the afterglow $[e] \sim (1-5) \cdot 10^{11}\,\text{cm}^{-3}$. The main attention is paid to the comparative analysis of the collisional-radiative recombination of Ne^{+} and Ne^{++} ions based on the numerical solution of coupled differential equations for the densities of charged and long-lived excited particles and the electron temperature, taking into account the main elementary processes in decaying neon plasma. Comparison of the model solutions with the intensities of ionic and atomic spectral lines measured by the multichannel photon counting method indicates the need to refine the dependence of the rate of collisional-radiative recombination on the ion charge.

Keywords: dielectric barrier discharge, doubly charged ions, collisional-radiative recombination, decaying plasma, elementary processes.

DOI: 10.21883/EOS.2022.07.54720.3077-21

Introduction

The present study is a continuation of the research into processes occurring in decaying plasma of a barrier discharge (DBD) [1,2]. This research is focused on analyzing the ionic line emission produced under a neon pressure lower than 1 Torr due to the collisional–radiative recombination of Ne^{++} ions. This emission enriches appreciably the plasma spectrum, which is formed by the processes of recombination of Ne_2^{+} and Ne^{+} ions with electrons, at lower pressures and becomes dominant in the violet region in the early afterglow, but disappears much faster as time passes. The mechanisms of recombination of Ne^{+} and Ne^{++} ions are identical:

$$Ne^{+} + e + e \xrightarrow{\alpha_{1cr}} Ne^{*} + e, \qquad (1)$$

$$Ne^{+} + e + e \xrightarrow{\alpha_{2cr}} Ne^{+*} + e. \qquad (2)$$

According to the theory of the process [3], the only difference is that a highly excited electron of a Ne^{+*} ion interacts more efficiently with plasma electrons and thus diffuses faster in the energy space „down“ to the ground ion state, finalizing an individual recombination event. In accordance with [3], recombination coefficients (1) and (2) in the limit of pure collisional kinetics of excited electrons do not depend on the ion type and differ only in factor Z^3, where Z is the ion charge that is equal to 2 in the present case: $\alpha_{2cr} = 8\alpha_{1cr}$.

Collisional–radiative recombination (1) is one of the key mechanisms of deionization of a wide spectrum of plasma objects. It has been examined in a number of experimental and theoretical studies (some of them were mentioned in [2]), which provide a fairly detailed insight into the process and provide an opportunity to model it at different degrees of ionization. The only available pieces of information on process (2) are the above-mentioned $\alpha_{Zcr} \sim Z^3$ [3] relation and the numerical solution of the problem [4] with account for radiative transitions in the kinetics of excited atoms. According to this solution, power R of Z may assume, depending on the density and temperature of plasma electrons, a value ranging from $R = 4$ to negative numbers.

Papers [5,6] are the only ones of note in the context of experimental investigation of the role of recombination of multicharged ions in shaping the properties of decaying plasma. The authors of these studies observed the afterglow of low-pressure ($P_{He} < 2$ Torr) helium plasma produced by a pulsed beam of monoenergetic electrons. The analysis of the mechanism of decay of ionic line intensities performed in [5,6] was restricted to a single hypothesis of destruction of He^{++} ions in collisions with metastable helium atoms; no data on recombination processes were obtained.

The aim of the present study is to model the behavior of intensities of atomic and ionic neon lines at the plasma decay stage and acquire data on the rate of collisional–radiative recombination of neon ions with charge $Z = 2$.

The following factors make such a study feasible.

1. Experiments reveal (see below) a clear dependence of the rate and nature of decay of intensities $J_i(t)$ of ionic lines in the afterglow on the plasma electron density.

2. Since the afterglow in ionic and atomic spectra is detected in the same conditions, plasma parameters and rate constants of elementary processes corresponding to the optimum characterization of lines of an atomic spectrum may be used to model the behavior of ionic lines.

3. Plasma with a complex ionic composition, which is the one produced in the discussed experiment and which contains atomic (Ne^{+}, Ne^{++}) and molecular (Ne_2^{+}) ions, features a clear distinction between the mechanisms of population of excited atom levels: the exit channels of dissociative recombination in decaying plasma

$$Ne_2^{+} + e \xrightarrow{\alpha_j} Ne_j^{*} + Ne \qquad (3)$$

contain only those atom levels (this is also true for atoms of other heavy inert gases) that lie below the ground vibrational level of a molecular ion on the energy scale. This is illustrated most vividly by the $2p^5 4p$ configuration levels of a neon atom [7]: spectral line intensities $J(t)$ emitted by the upper four $4p$ levels are proportional to recombination flux (1), while the population of the remaining six levels is related to dissociative recombination (3).

The formation of collisional–radiative recombination flux (1) in the conditions of the discussed experiment with relatively low electron densities, which are insufficient for a purely collisional [3] process, is characterized by an intermediate model: the rate constant of the process is specified by the collisional kinetics of highly excited atoms, while the recombination flux in the space of levels with small principal quantum numbers (estimates were presented in [2]) is borne primarily by radiation.This makes it possible to analyze the process based on the results of spectroscopic observations.

Experimental procedure and results

Plasma was produced by a low-frequency (80 Hz) barrier discharge in a cylindrical glass tube (Fig. 1) with a length of 20 cm and a diameter of 3.9 cm. The characteristic features of plasma of such a discharge were detailed in [1,2]. The degree of ionization of gas in the setup in Fig. 1 may be adjusted simply by varying the duration of voltage pulse T_p that switches transistor Tr on and sets the energy stored in the primary winding of flyback transformer T. This energy is transferred to the secondary winding when the transistor is switched off. The secondary winding current in this setup has the shape of two half-waves of different polarities, each of which has a duration of several microseconds. With ratio $N_2/N_1 = 10$ of numbers of turns and neon pressures lower than 200 Torr, the discharge tube of the indicated size could produce plasma with axial electron density $[e] \sim 10^{10}–5 \cdot 10^{11}\,cm^{-3}$. The induction high-frequency discharge (RF Pulse) spiral wound on top of the DBD electrodes was used for pulsed „heating“ of electrons of decaying plasma that was needed for two purposes: examine the response of intensities of spectral lines and estimate the density of electrons in the afterglow

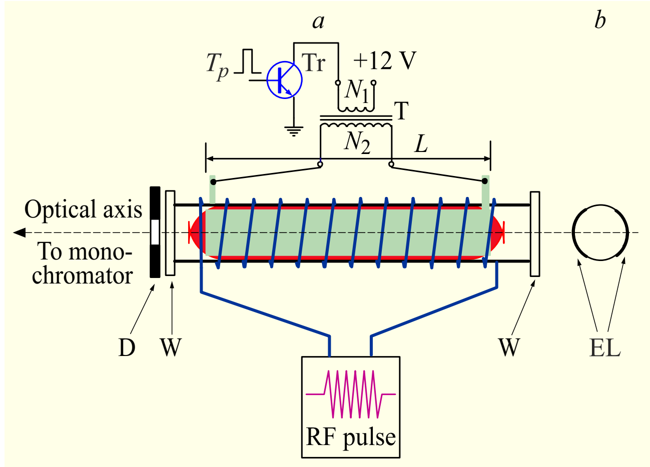

Figure 1. (*a*) Diagram of the setup used to combine barrier and pulsed HF discharges (RF Pulse): D is an aperture 5 mm in diameter, and W are quartz windows. (*b*) Positioning of DBD electrodes (EL) on the side surface of a discharge tube.

based on the response of Ne $2p^5 3s(^3P_1)$ atom population to the electron temperature variation [1,2]. The factors affecting the electron temperature in the afterglow of low-pressure neon plasma were analyzed in [2]. In addition, the afterglow with „heating“ of electrons in the context of prevalence of ambipolar diffusion in the plasma decay was modeled in this study. It was found, among other things, that a rate of process (2) higher than the one specified by the theory [3] is better suited for the model.

The present study is focused on the results of a spectroscopic experiment that demonstrates the variation of line intensities proportional to recombination fluxes (1) and (2) at different stages of the afterglow and different DBD powers corresponding to electron densities $[e] \approx (1–5.5)10^{11}\,cm^{-3}$ at the tube axis. Since the electron densities at the late afterglow were lower than $10^{10}\,cm^{-3}$, long signal accumulation times (from several minutes to several hours) and fairly wide entrance and exist slits of the monochromator, which had a spectral width of $\Delta\lambda \sim 0.2$ nm, were needed to measure the intensities in a wide dynamic range. The 576.4 nm line was used as a probing tool for examining the recombination of Ne^{+} ions. Its upper $4d$ level is located ~ 0.45 eV higher than the ground vibrational level of a Ne_2^{+} ion. Process (2) was analyzed based on the results of monitoring of plasma emission at a wavelength around 334.5 nm; thus, ionic lines with wavelengths of 334.4, 334.5, and 334.6 nm fell within the $\Delta\lambda$ interval.

Some of the results of the experiment are presented in Fig. 2. It can be seen that ionic $J_i(t)$ and atomic $J_a(t)$ lines differ considerably in their behavior at all experimental conditions. At low electron densities, when recombination plays only a minor role in the plasma decay, this difference is associated, first, with the charge transfer from Ne^{++} ions in collisions with neon atoms

$$Ne^{++} + Ne \xrightarrow{k_+} Ne^+ + Ne^+, \tag{4}$$

(the data on rate constant k_+ of process (4) obtained experimentally [8,9] differ several-fold: $9 \cdot 10^{-14}\,cm^3s^{-1}$ in [8] and around $2 \cdot 10^{-14}\,cm^3s^{-1}$ in [9]) and, second, with a more than 1.5-fold difference between ambipolar diffusion coefficients of Ne^+ and Ne^{++} ions [8–10].

The variation of nature of temporal dependences of line intensities (normalized to the same measurement conditions in Fig. 2) with growth of the initial electron density indicates clearly that the contribution of recombination processes (1), (2) to the plasma decay increases.

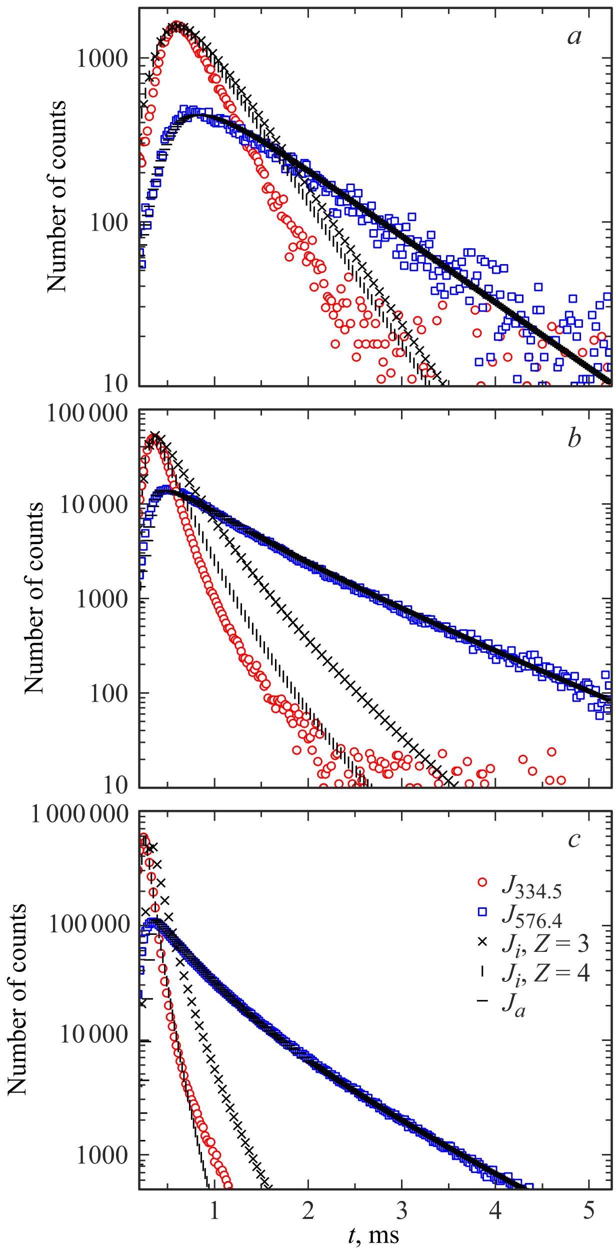

Figure 2. Intensities of spectral lines and model curves for initial electron densities $[e] \sim 10^{11}$ (a), $2.9 \cdot 10^{11}$ (b), $5.5 \cdot 10^{11}\,cm^{-3}$ (c). The neon pressure is 0.65 Torr, $t = 0$ corresponds to the onset of DBD.

Afterglow model

The intensities of lines related to processes (1), (2) were considered to be proportional to the number of recombination events:

$$J_a(t) \sim \alpha_{1cr}(T_e)[e][Ne^+], \tag{5}$$

$$J_i(t) \sim \alpha_{2cr}(T_e)[e][Ne^{++}]. \tag{6}$$

Let us first discuss the results of simulation of plasma emission at transitions in the atomic spectrum. We used the following approximation from [11] of the dependence of collisional–radiative recombination coefficient α_{1cr} on plasma parameters:

$$\alpha_{1cr} = 1.55 \cdot 10^{-10} T_e^{0.63} + 6.0 \cdot 10^{-9} T_e^{2.18} [e]^{0.37} + 3.8 \cdot 10^{-9} T_e^{4.5} [e]. \tag{7}$$

Here, T_e is the electron temperature in kelvins, $[e]$ is expressed in cm^{-3}, and α_{1cr} is expressed in cm^3s^{-1}. The last term in (7) is the recombination coefficient in the case of purely collisional kinetics of excited electrons (matches the one calculated in [3] in the sense of dependence on plasma parameters and close in absolute value at $Z = 1$), while the first term characterizes the process in weakly ionized plasma (radiative recombination).

The model used to characterize the experimental data was discussed in detail in [2]) and contains a large set of rate constants of elementary processes affecting the evolution of plasma parameters in the afterglow. In view of this, one cannot find a solution fitting the experimental results so closely as the model curves in Fig. 2 do by inserting these constants, which were measured with a certain error or calculated (e.g., rate of electron-ion collisions $\nu_{ei}(T_e)$) using approximate formulae, into the system of differential equations of the model (seven equations for densities of ions, atoms in metastable and resonance states, and electron temperature). In addition, the plasma parameters crucial to this problem (temperature and density of electrons at the early afterglow stage), which are used as the initial conditions in the system of equations, were also determined with a limited accuracy. For example, our estimates [2] demonstrate that the error of determination of electron density $[e](t_r)$ at the reference afterglow point ($t_r \sim 1.5$ ms) based on the response of the population of neon atoms in the $2p^53s(^3P_1)$ state to pulsed „heating" of electrons is no lower than 30%. Therefore, it turned out to be impossible to bring the solution calculated based on $[e](t_r)$ closer to the experimental curves even by varying other model parameters within reasonable limits. Model $J_a(t)$ curves in Fig. 2 were plotted in two stages in the following way. Model parameters from [2], which specify the conditions in which the data in Fig. 2, a were obtained, were used as a first

Model electron densities at the onset of the afterglow $[e]_M(t_0)$, at the maximum $J_a(t)$ intensity $[e]_M(t_{max})$, and at a reference point $[e]_M(t_r)$; electron temperature at the onset of the afterglow $T_e(t_0)$; and fraction of energy δ transferred by „fast“ electrons to the main group of plasma electrons. Lines *a*, *b*, and *c* correspond to Figs. 2, *a*, *b*, and *c*

	$[e]_M(t_0)$	$[e]_M(t_{max})$	$[e](t_r)$, $[e]_M(t_r)$	$T_e(t_0)10^3$ K	δ	$[Ne^{++}]/[Ne^{+}]$
a	1	0.44	0.4, 0.32	45	0.25	0.3
b	2.9	1.3	0.8, 0.72	60	0.35	0.37
c	5.5	2.2	1.2, 0.91	70	0.4	0.5

approximation. To achieve the best fit to experimental data, two parameters (electron density $[e](t_0)$ at the onset of the afterglow and scale factor *m*) were adjusted for aligning the calculated curve with the experimental intensities at their maxima: $J_a(t) = m\alpha_{1cr}(T_e)[e][Ne^{+}]$.

The temporal variation of intensities $J_a(t)$ and $J_i(t)$ depends (although only slightly) on relative ion density $[Ne^{++}]/[Ne^{+}]$, which was estimated at ~ 0.3 in [2]. This estimate was used as a first approximation. Certain parameters of the model are listed in the table.

It is important to note that the search for the optimum model parameters for the entire set of experimental data was performed with the same unchanged set of rate constants of elementary processes (the one found for Fig. 2, *a*). The fit between experimental and calculated curves was achieved by adjusting $[e](t_0)$ and factor *m*. Note that the variation of $J_a(t)$ (and especially $J_i(t)$) became affected more and more strongly by the term in the equation for $T_e(t)$ proportional to frequency $\nu_{ei}(T_e)$ (it was taken into account in the calculation of ν_{ei} that the cross section of the electron–ion interaction is proportional to Z^2) as $[e](t_0)$ increased. When the relaxation rate of electron energy in the afterglow increased, the $J_a(t)$ maximum shifted somewhat from the experimental points toward the origin of coordinates. Their realignment required increasing temperature $T_e(t_0)$ and (or) the fraction of energy (δ in the table) transferred by „fast“ electrons, which are produced in reactions involving neon atoms in resonance and metastable states, to plasma electrons. The final values of these parameters were determined at the closing stage of processing in joint analysis of $J_a(t)$ and $J_i(t)$. These values are the ones listed in the table.

Constructing the model of recombination of double-charged ions, we relied on the conclusions made in [3], where the $\alpha_{Zcr} \sim Z^3$ relation was found, and the results of the already mentioned measurements [8–10] of the rate constant of process (4) and the mobility of Ne^{++} in neon. The third term in formula (4) with coefficient $Z^3 = 8$ was used as the recombination coefficient:

$$\alpha_{2cr} = 8 \cdot 3.8 \cdot 10^{-9} T_e^{4.5} [e], \quad (8)$$

and the remaining parameters (including the initial values of $[e](t_0)$ and $T_e(t_0)$) were borrowed from the results of simulation of $J_a(t)$. The scaling factor, which was adjusted so as to align the calculated data with the experimental ones in the vicinity of the maximum intensity of a line, was the only fitting parameter. The results (Fig. 2) revealed that the obvious discrepancy between decay rates $J_i(t)$ and $J_{334.5}(t)$ cannot be rectified by any variation of the problem parameters without disturbing fundamentally the alignment between $J_a(t)$ and $J_{576.4}(t)$ under any experimental conditions (Fig. 2 presents only a fraction of the studied regimes). The sole exception is the enhancement of the diffusion rate of Ne^{++}, which is unsubstantiated (the data from [8] and [9] are close), and (or) the rate constant of process (4). The latter was done by inserting the value of $9 \cdot 10^{-14}\,\mathrm{cm^3s^{-1}}$ proposed in [8]. This did indeed produce a better fit between $J_i(t)$ and $J_{334.5}(t)$ at the minimum experimental value of the electron density (Fig. 2, *a*). However, at higher $[e]$ values, $J_{334.5}(t)$ became qualitatively inconsistent with the experimentally observed reduction of the decay rate of ionic line intensities with time, bringing this decay closer to a purely exponential one. Just as in [2], we used constant $k_+ = 3.7 \cdot 10^{-14}\,\mathrm{cm^3s^{-1}}$ in the model.

It is worth emphasizing that the evident discrepancies between $J_i(t)$ and $J_{334.5}(t)$ and the almost ideal fit between $J_a(t)$ and $J_{576.4}(t)$ are not related to the apparent incorrectness of the approach to the description of atomic and ionic spectra with formulae (7) (valid for arbitrary electron densities) and (8) (corresponds to purely collisional kinetics of excited electrons). The case is that the third term in (7) already produces the dominant contribution to $J_a(t)$ in the conditions represented in Fig. 2, *b* (and certainly in Fig. 2, *c*). Thus, the only way to bring $J_i(t)$ closer to $J_{334.5}(t)$ is to raise the model recombination rate of double-charged ions. With this aim in view, we performed calculations with recombination coefficient

$$\alpha_{2cr} = 16 \cdot 3.8 \cdot 10^{-9} T_e^{4.5} [e], \quad (9)$$

which corresponds to dependence $\alpha_{Zcr} \sim Z^4$. The calculation results are presented in Fig. 2. For ease of comparison, we did also adjust the scaling factor in this case, aligning the calculation results with the data for Z^3 at the $J_i(t)$ maximum. It can be seen that, following the transition to Z^4, the calculated curves become closer to the experimental data as the electron density increases, although the goodness of fit is still fairly far from the one achieved for the 576.4 nm line. The discrepancy between the dependences of calculated and observed decay rates of the ionic line on plasma parameters, which vary with time in the afterglow, is also noticeable (especially in Fig. 2, *c*). This discrepancy at large times could possibly be eliminated by raising $J_i(t)$:

adding terms, which factor in the deviation from the purely collisional recombination model, to α_{2cr}, as was done in (7). However, as far as we know, this approach has not been implemented for double-charged ions.

We note the following in relation to the plasma parameters at the right-hand side of the table. Varying parameters $T_e(t_0)$ and δ, we observed somewhat different, but close changes in the solution for $J_i(t)$. Therefore, the sought-for quantities turned out to be interdependent. Thus, the tabulated data should be understood as a manifestation of the trend toward an increase in these parameters at higher DBD powers rather than as a sign of the possibility of their determination in a purely spectroscopic experiment. This is also true for the relative density of ions.

Conclusion

The feasibility of characterization of the evolution of line intensities in atomic and ionic spectra in the afterglow with the electron density varying within the $[e] \sim (0.1-5) \cdot 10^{11}\,\mathrm{cm}^{-3}$ range based on the numerical solution of a system of coupled first-order differential equations, which factor in the key processes involving charged and long-lived excited particles, was demonstrated. It was found that the model parameters providing an almost ideal fit between the calculated and experimental intensities of spectral lines of a neon atom do not render an adequate characterization of the afterglow of ionic lines. It was demonstrated that ionic lines are modeled much more fittingly if the coefficient of collisional–radiative recombination of double-charged ions is increased by a factor of at least 2 relative to its value adopted in the current concepts of the process.

Conflict of interest

The author declares that he has no conflict of interest.

References

[1] V.A. Ivanov. Plasma Sources Sci. Technol., **29**, 045022 (2020). 10.1088/1361-6595/ab7f4c
[2] V.A. Ivanov. Opt. Spectrosc., **129** (10), 1104 (2021). DOI: 10.1134/S0030400X21080099
[3] A.V. Gurevich, L.P. Pitaevskii. Sov. Phys. JETP, **19** (4), 870 (1964).
[4] D.R. Bates, A.E. Kingston, R.W.P. McWhirter. Proc. Roy. Soc. (London), A267, 297 (1962). https://www.jstor.org/stable/2414257
[5] O.V. Zhigalov, Yu.A. Piotrovskiĭ, Yu.A. Tolmachev. Opt. Spectrosc., **97** (2), 167 (2004). DOI: 10.1134/1.1790631.
[6] O.V. Zhigalov, Yu.A. Piotrovskiĭ, Yu.A. Tolmachev. Opt. Spectrosc., **97** (5), 673 (2004). DOI: 10.1134/1.1828614.
[7] S.V. Gordeev., V.A. Ivanov, Yu.E. Skoblo. Opt. Spectrosc., **127** (3), 418 (2019). DOI: 10.1134/S0030400X19090133.
[8] F.J. de Hoog, H.J. Oskam. J. Appl. Phys., **44**, 3496 (1973).
[9] R. Johnsen, M.A. Biondi. Phys. Rev. A., **18** (3), 989 (1978).
[10] G.E. Courville, M.A. Biondi. J. Chem. Phys., **37** (3), 616 (1962).
[11] J. Stevefelt, J. Boulmer, J-F. Delpech. Phys. Rev. A, **12** (4), 1246 (1975).